

Metal-insulator transition and lattice instability of paramagnetic V₂O₃I. Leonov,¹ V. I. Anisimov,^{2,3} and D. Vollhardt¹¹*Theoretical Physics III, Center for Electronic Correlations and Magnetism, Institute of Physics, University of Augsburg, 86135 Augsburg, Germany*²*Institute of Metal Physics, Sofia Kovalevskaya Street 18, 620990 Yekaterinburg GSP-170, Russia*³*Department of Theoretical Physics and Applied Mathematics, Ural Federal University, 620002 Yekaterinburg, Russia*

(Received 27 October 2014; revised manuscript received 15 April 2015; published 11 May 2015)

We determine the electronic structure and phase stability of paramagnetic V₂O₃ at the Mott-Hubbard metal-insulator transition (MIT) by employing a combination of an *ab initio* method for calculating band structures with dynamical mean-field theory. The structural transformation associated with the MIT occurs upon a slight expansion of the lattice volume by $\sim 1.5\%$, in agreement with experiment. Our results show that the structural transition precedes the MIT, implying a complex interplay between electronic and lattice degrees of freedom. The MIT is found to be driven by a strong correlation-induced, orbital-selective renormalization of the V t_{2g} bands. The effective electron mass of the e_g^π orbitals diverges at the MIT. Our results show that full charge self-consistency is crucial for a correct description of the physical properties of V₂O₃.

DOI: 10.1103/PhysRevB.91.195115

PACS number(s): 71.10.-w, 71.27.+a

I. INTRODUCTION

The question concerning the nature of a Mott metal-insulator phase transition (MIT) poses one of the most fundamental problems in condensed-matter physics. It becomes an even greater challenge in the case of materials with a strong interplay between electronic correlations and lattice degrees of freedom. The most famous example is V₂O₃, which has generally been considered to be the classical example of a material with a Mott-Hubbard MIT [1]. Under ambient conditions, V₂O₃ is a paramagnetic metal with a corundum crystal structure (space group $R\bar{3}c$) [2,3]. Upon doping with Cr it undergoes a phase transition to a paramagnetic Mott-Hubbard insulator without change of crystal symmetry [4]. The transition from the paramagnetic insulator (PI) to the paramagnetic metal (PM) can also be triggered by doping with Cr, which essentially amounts to the application of a negative pressure. The MIT is intimately linked with an abrupt expansion of the lattice volume by $\frac{\Delta V}{V} \sim 1.3\%$ and a reduction of the c/a lattice parameter ratio by $\sim 1.4\%$ across the MIT, indicating a strong coupling between electronic and lattice degrees of freedom [4]. In spite of intensive research over several decades, an explanation of this mutual influence of electronic structure and phase stability of paramagnetic V₂O₃ at the MIT is still missing. Therefore investigations of V₂O₃ continue with a high level of activity [5,6].

A realistic description of V₂O₃ requires taking into account the interplay of electronic correlations and lattice degrees of freedom on a microscopic level. State-of-the-art methods for the calculation of the band structure, which allow for *ab initio* computations of the electronic and structural properties, can account for neither the MIT nor the paramagnetic insulating phase of V₂O₃ [7]. This obstacle can be overcome by employing the LDA/GGA+DMFT approach [8], a combination of band-structure methods in the local-density approximation (LDA) or the generalized gradient approximation (GGA) with dynamical mean-field theory (DMFT) of strongly correlated electrons [9]. Applications of LDA+DMFT have already provided a good quantitative description of the electronic structure and spectral properties of V₂O₃ [6,10–15]. In

particular, it was found that in all phases the V³⁺ ions are in a $S = 1$ spin configuration, with a mixed (a_{1g} , e_g^π) and (e_g^π , e_g^π) orbital occupation. These calculations also allow one to perform a direct comparison of the calculated spectra with, e.g., photoemission, x-ray absorption, and optical conductivity measurements near the metal-insulator transition [6,10–15]. The LDA+DMFT results capture all generic aspects of a Mott-Hubbard metal-insulator transition, such as a coherent quasiparticle behavior, formation of the lower and upper Hubbard bands, and strong renormalization of the effective electron mass. In addition, these calculations reveal an orbital-selective behavior of the electron coherence and a strong enhancement of the crystal-field splitting between the a_{1g} and e_g^π bands, caused by electron correlations at the MIT [10,12]. Despite this success the coupling between electronic correlations and lattice structure at the Mott-Hubbard MIT in V₂O₃ is still poorly understood. We will address this problem in our investigation and thereby shed new light on the long-standing question regarding the origin of the structural changes in the vicinity of the MIT.

II. METHOD

In this paper we employ the GGA+DMFT computational approach [16] to explore the electronic and structural properties of paramagnetic V₂O₃ across the Mott-Hubbard MIT. In particular, we will explore the structural phase stability of paramagnetic V₂O₃, i.e., the influence of electronic correlations on the *structural* transition. We first compute the electronic structure of paramagnetic V₂O₃ within the nonmagnetic GGA using the plane-wave pseudopotential approach [17]. To investigate the structural stability, we use the atomic positions and the c/a lattice parameter ratio of V₂O₃ taken from experiment [4]. To this end, we adopt the crystal structure data for paramagnetic metallic V₂O₃ and insulating (V_{0.962}Cr_{0.038})₂O₃, respectively, and calculate the total energy as a function of volume. In Fig. 1 (inset) we show the results of the nonmagnetic GGA total-energy calculations, which agree with previous band-structure results [7]. In particular, we find

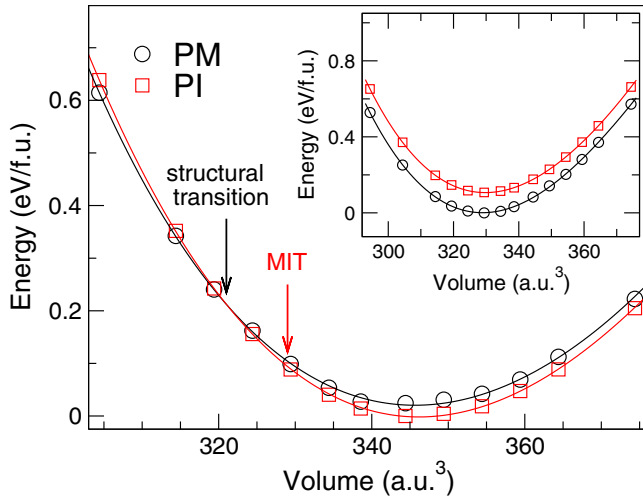


FIG. 1. (Color online) Variation of the total energy of paramagnetic V_2O_3 computed within GGA+DMFT for different volumes. The inset shows the results of the nonmagnetic GGA total-energy calculations.

equilibrium lattice constants $a = 4.923 \text{ \AA}$ for the PM phase and 4.955 \AA for the PI phase of V_2O_3 . The calculated bulk moduli are $B \sim 252 \text{ GPa}$ for both phases. These results are in neither quantitative nor even qualitative agreement with experiment. Namely, they give a metallic solution with no structural phase transition between the PM and PI phases. Clearly, standard band-structure techniques cannot explain the properties of paramagnetic V_2O_3 since they do not treat electronic correlations adequately.

III. RESULTS AND DISCUSSION

A. Non-self-consistent calculations

Therefore we now compute the electronic structure and phase stability of V_2O_3 using the GGA+DMFT computational scheme [16]. For the partially filled V t_{2g} orbitals, which split into a_{1g} and e_g^π bands due to a trigonal distortion, we construct a basis of atomic-centered symmetry-constrained Wannier functions [18]. To solve the realistic many-body problem within DMFT, we employ the continuous-time hybridization-expansion quantum Monte Carlo algorithm [19,20]. The calculations are performed at the temperature $T \sim 390 \text{ K}$, which is below the critical end point of $T_c \sim 458 \text{ K}$ [21]. We use values of the Coulomb interaction $U = 5 \text{ eV}$ and Hund's exchange $J = 0.93 \text{ eV}$, in accordance with the previous theoretical and experimental estimations [6,10–12]. The U and J values are assumed to remain constant across the phase transition, which is consistent with recent hard x-ray photoemission experiments [22]. Furthermore we employ the fully localized double-counting correction, calculated from the self-consistently determined local occupancies, to account for the electronic interactions already described by the GGA.

In Fig. 1 (main panel) we display the calculated variation of the total energy of paramagnetic V_2O_3 as a function of lattice volume. Our results for the equilibrium lattice constant and bulk modulus, which now include the effect of electronic correlations, agree well with experiment [4]. The calculated

equilibrium lattice constants are $a = 5.005$ and 5.035 \AA for the PM and PI phases, respectively. The corresponding bulk moduli are $B = 202$ and 222 GPa . In agreement with previous studies [10,12], our results show an orbital dependence of the electron coherence, with coherent quasiparticle behavior for the a_{1g} orbital, while the e_g^π bands remain incoherent, with a large imaginary part of the self-energy at $T \sim 390 \text{ K}$. We also evaluated the spectral function of paramagnetic V_2O_3 (not shown here) and determined the MIT phase boundary. The MIT is found to take place at a positive pressure of $p_{el} \sim 125 \text{ kbar}$, implying a $\frac{\Delta V}{V} \sim 5\%$ reduction of the lattice volume. We find that both the a_{1g} and the e_g^π quasiparticle weights remain finite at the MIT; that is, there is *no* divergence of the effective electron mass at the transition as it would occur in a Brinkman-Rice picture of the MIT [23]. Thus we conclude that the MIT is driven by a strong enhancement of the a_{1g} - e_g^π crystal-field splitting caused by electron correlations [10,12].

The GGA+DMFT results are qualitatively different from those obtained with the nonmagnetic GGA and provide clear evidence for a structural phase transition. However, this transition is found to occur at a critical pressure of $p_c \sim 186 \text{ kbar}$, corresponding to a large ($\sim 7\%$) reduction of the lattice volume. In addition, the results imply that the PM phase is energetically unfavorable at ambient pressure, i.e., thermodynamically unstable, with a total-energy difference with respect to the PI phase of $\Delta E \equiv E_{PM} - E_{PI} \sim 20 \text{ meV/f.u.}$ These features are in contrast to experiment. The origin of this discrepancy can be ascribed to the lack of charge self-consistency in the present calculations. Indeed, a strong enhancement of the a_{1g} - e_g^π crystal-field splitting will cause a substantial redistribution of the charge density and thereby influence the lattice structure due to electron-lattice coupling. All this makes charge self-consistency [24] particularly important at the metal-insulator transition.

B. Self-consistent calculations

For this reason we implemented a fully charge self-consistent GGA+DMFT method [24] within a plane-wave pseudopotential approach to compute the electronic structure and phase stability of V_2O_3 . In Fig. 2 we present our results for the total energy for different volumes. The calculated pressure-volume equation of state is shown in Fig. 2 (inset). The PM phase is now found to be thermodynamically stable at ambient pressure, with a total-energy difference between the PM and PI phases of $\Delta E \sim 3 \text{ meV/f.u.}$ The structural transition takes place upon a slight expansion of the lattice, $\frac{\Delta V}{V} \sim 1.5\%$, at a negative critical pressure of $p_c \sim -28 \text{ kbar}$, in agreement with experiment. The phase transition is accompanied by an abrupt increase of the lattice volume by $\sim 0.5\%$ and a simultaneous change of the c/a ratio by $\sim 1.5\%$. This result is seen to differ significantly from that obtained with the non-charge-self-consistent GGA+DMFT scheme, according to which the PM phase is thermodynamically unstable at ambient pressure. The calculated equilibrium lattice constants and bulk moduli are now in remarkably good agreement with experiment [4]. In particular, we obtain $a = 4.99$ and 5.021 \AA for the PM and PI phases, respectively, which is less than 1% larger than the experimental values. The calculated bulk moduli are $B = 219$ and 204 GPa , respectively. We note that the bulk modulus in the

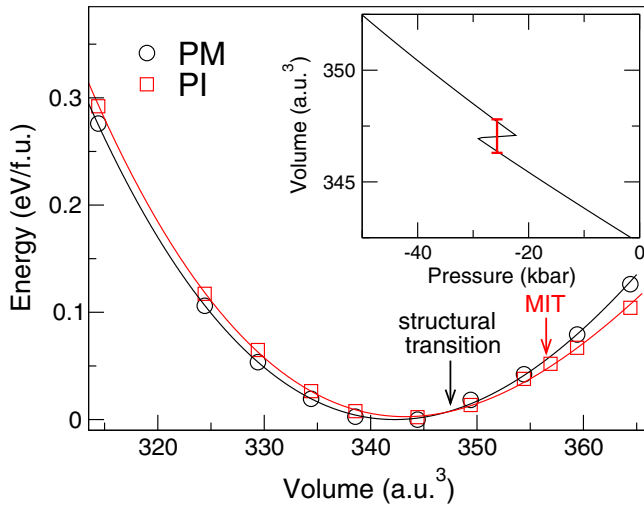


FIG. 2. (Color online) Variation of the total energy of paramagnetic V_2O_3 as a function of volume obtained by employing the fully charge self-consistent GGA+DMFT method. The inset shows the corresponding volume-pressure equation of state obtained as a derivative of the spline interpolation of $E(V)$. The calculated critical pressure $p_c \sim -28$ kbar and volume collapse by $\sim 0.5\%$ are marked by a red bar.

PI phase is somewhat smaller than that in the PM phase, which implies an *enhancement* of the compressibility at the phase transition. Furthermore, the total-energy calculation results exhibit a weak anomaly near the MIT, which is associated with a divergence of the compressibility, in accordance with previous model calculations [25]. Overall, the electronic structure, the equilibrium lattice constant, and the structural phase stability of paramagnetic V_2O_3 obtained with the fully charge self-consistent GGA+DMFT scheme are in remarkably good agreement with the experimental data. Our calculations clearly demonstrate the crucial importance of electronic correlations and full charge self-consistency to explain the thermodynamic stability of the paramagnetic metal phase of V_2O_3 .

C. Spectral function

In addition, we investigated the evolution of the spectral function of paramagnetic V_2O_3 . In Fig. 3 we present our results obtained with the fully charge self-consistent GGA+DMFT approach for paramagnetic V_2O_3 across the MIT. Our calculations show that the V^{3+} ions are in a $S = 1$ spin configuration in all phases, with a predominant occupation of the e_g^π bands and substantial admixture of the a_{1g} orbital. The admixture is almost independent of changes of the lattice volume (deviations $< 5\%$), with a small decrease at the structural transition. Our results for the (a_{1g}, e_g^π) orbital occupations at the phase transition are $(0.44, 0.78)$ for the PM phase and $(0.42, 0.79)$ for the PI phase of V_2O_3 . These findings are in good agreement with previous experimental estimations [26]. We note that the MIT takes place at a negative pressure $p_{el} \sim -66$ kbar, i.e., upon an expansion of the lattice volume by $\sim 2\%$, above the structural phase transition. Thereby we conclude that the structural transition and the electronic transition are *decoupled*. Apparently, the structural transformation occurs as a precursor to the Mott-Hubbard MIT

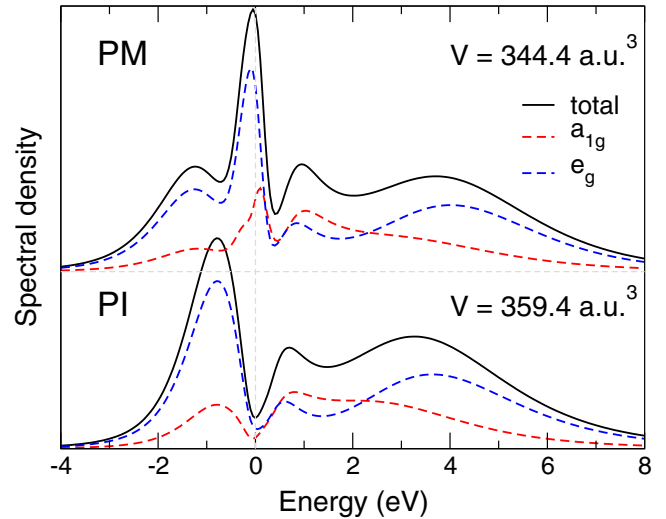


FIG. 3. (Color online) Spectral function of paramagnetic V_2O_3 across the MIT computed within GGA+DMFT.

[27], implying an intricate interplay between electronic and lattice degrees of freedom at the transition.

D. Quasiparticle weight

Finally, we calculate the quasiparticle weight employing a polynomial fit of the imaginary part of the self-energy $\text{Im}\Sigma(i\omega_n)$ at the lowest Matsubara frequencies ω_n . It is evaluated as $Z = [1 - \partial\text{Im}\Sigma(i\omega)/\partial i\omega]^{-1}$ from the slope of the polynomial fit at $\omega = 0$. In Fig. 4 we present our results for the a_{1g} and e_g^π quasiparticle weights evaluated for the PI phase. Upon lattice volume expansion, both the a_{1g} and e_g^π quasiparticle weights monotonously decrease. Moreover, in the vicinity of the MIT the a_{1g} quasiparticle weight remains finite, while $Z = 0$ for the e_g^π orbitals, i.e., $\text{Im}\Sigma(\omega)$ diverges for $\omega \rightarrow 0$. Therefore we conclude that the electronic effective

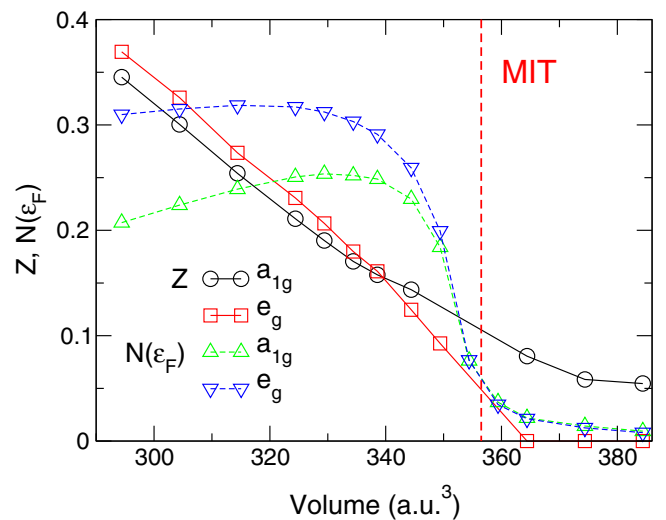


FIG. 4. (Color online) Quasiparticle weight Z and spectral weight at the Fermi level $N(\epsilon_F) = -\frac{\beta}{\pi}G(\tau = \beta/2)$ obtained for the a_{1g} and e_g^π orbitals across the MIT in the PI phase of V_2O_3 . The MIT itself is indicated by a red dashed line.

mass of the e_g^π bands diverges at the MIT, in agreement with thermodynamic measurements of V_2O_3 [28]. We note that this divergence coincides with the drop of the spectral weight for the a_{1g} and e_g^π orbitals at the Fermi level shown in Fig. 4. The MIT is therefore driven by a strong orbital-selective renormalization of the V t_{2g} bands, in accordance with a Brinkman-Rice picture of the MIT. These results correct previous reasonings based on a correlation-induced enhancement of the crystal-field splitting of the V t_{2g} manifold, which results in a suppression of the hybridization between the a_{1g} and e_g^π bands [10,12]. On this basis, we conclude that an orbital-selective Mott transition is the only viable scenario for the MIT in V_2O_3 .

IV. CONCLUSION

In conclusion, we employed the GGA+DMFT computational approach to determine the electronic structure and phase stability of paramagnetic V_2O_3 across the Mott-Hubbard metal-insulator phase transition. The calculated structural phase stability and spectral properties are in good agreement with experiment. Full charge self-consistency is found to be crucial to obtain the correct equilibrium lattice and electronic structure of V_2O_3 at ambient pressure. Upon lattice expansion, a structural phase transition is found to take place at $p_c \sim -28$ kbar, in agreement with experiment. The phase

transition is accompanied by an abrupt lattice volume expansion by $\sim 0.5\%$ and a simultaneous change of the c/a lattice parameter ratio by about 1.5%. Our calculations reveal an orbital-selective renormalization of the V t_{2g} bands caused by strong electron correlations. The electronic effective mass of the e_g^π orbitals diverges at the MIT, in accordance with a Brinkman-Rice picture of the MIT. However, the a_{1g} orbital exhibits a finite quasiparticle weight across the MIT. We therefore conclude that an orbital-selective Mott transition is the only viable scenario for the MIT in V_2O_3 . Most importantly, we find that the structural transformation is decoupled from the electronic MIT. Our findings highlight the subtle interplay between electronic correlations and lattice stability across the Mott-Hubbard MIT.

ACKNOWLEDGMENTS

We thank F. Lechermann and A. I. Poteryaev for valuable discussions. Support from the Deutsche Forschungsgemeinschaft through TRR 80 (I.L.) and FOR 1346 (D.V.) is gratefully acknowledged. V.I.A. acknowledges support from the Russian Scientific Foundation (Project No. 14-22-00004), the Russian Foundation for Basic Research (Project No. 13-02-00050), and the Ural Division of the Russian Academy of Science Presidium (Project No. 15-8-2-4).

-
- [1] N. F. Mott, *Rev. Mod. Phys.* **40**, 677 (1968); *Metal-Insulator Transitions* (Taylor and Francis, London, 1990); M. Imada, A. Fujimori, and Y. Tokura, *Rev. Mod. Phys.* **70**, 1039 (1998).
- [2] D. B. McWhan and T. M. Rice, *Phys. Rev. Lett.* **22**, 887 (1969).
- [3] Upon cooling below $T_N \sim 155$ K, V_2O_3 undergoes a first-order phase transition from a paramagnetic metal to an antiferromagnetic insulator, with a concomitant transformation to a monoclinic crystal structure ($I2/a$) [4].
- [4] D. B. McWhan, T. M. Rice, and J. P. Remeika, *Phys. Rev. Lett.* **23**, 1384 (1969); D. B. McWhan and J. P. Remeika, *Phys. Rev. B* **2**, 3734 (1970); D. B. McWhan, A. Menth, J. P. Remeika, W. F. Brinkman, and T. M. Rice, *ibid.* **7**, 1920 (1973).
- [5] Y. Ding, C.-C. Chen, Q. Zeng, H.-S. Kim, M. J. Han, M. Balasubramanian, R. Gordon, F. Li, L. Bai, D. Popov, S. M. Heald, T. Gog, H. K. Mao, and M. van Veenendaal, *Phys. Rev. Lett.* **112**, 056401 (2014); X. Deng, A. Sternbach, K. Haule, D. N. Basov, and G. Kotliar, *ibid.* **113**, 246404 (2014); L. Dillemans, T. Smets, R. R. Lieten, M. Menghini, C.-Y. Su, and J.-P. Locquet, *Appl. Phys. Lett.* **104**, 071902 (2014); J. S. Brockman, L. Gao, B. Hughes, C. T. Rettner, M. G. Samant, K. P. Roche, and S. S. P. Parkin, *Nat. Nanotechnol.* **9**, 453 (2014).
- [6] D. Grieger, C. Piefke, O. E. Peil, and F. Lechermann, *Phys. Rev. B* **86**, 155121 (2012); P. Hansmann, A. Toschi, G. Sangiovanni, T. Saha-Dasgupta, S. Lupi, M. Marsi, and K. Held, *Phys. Status Solidi B* **250**, 1251 (2013); D. Grieger and F. Lechermann, *Phys. Rev. B* **90**, 115115 (2014).
- [7] L. F. Mattheiss, *J. Phys. Condens. Matter* **6**, 6477 (1994).
- [8] V. I. Anisimov, A. I. Poteryaev, M. A. Korotin, A. O. Anokhin, and G. Kotliar, *J. Phys. Condens. Matter* **9**, 7359 (1997); A. I. Lichtenstein and M. I. Katsnelson, *Phys. Rev. B* **57**, 6884 (1998); K. Held, I. A. Nekrasov, G. Keller, V. Eyert, N. Blümer, A. K. McMahan, R. T. Scalettar, Th. Pruschke, V. I. Anisimov, and D. Vollhardt, *Phys. Status Solidi B* **243**, 2599 (2006); G. Kotliar, S. Y. Savrasov, K. Haule, V. S. Oudovenko, O. Parcollet, and C. A. Marianetti, *Rev. Mod. Phys.* **78**, 865 (2006); J. Kunes, I. Leonov, M. Kollar, K. Byczuk, V. I. Anisimov, and D. Vollhardt, *Eur. Phys. J. Spec. Top.* **180**, 5 (2010).
- [9] W. Metzner and D. Vollhardt, *Phys. Rev. Lett.* **62**, 324 (1989); A. Georges, G. Kotliar, W. Krauth, and M. J. Rozenberg, *Rev. Mod. Phys.* **68**, 13 (1996); G. Kotliar and D. Vollhardt, *Phys. Today* **57**(3), 53 (2004).
- [10] K. Held, G. Keller, V. Eyert, D. Vollhardt, and V. I. Anisimov, *Phys. Rev. Lett.* **86**, 5345 (2001); G. Keller, K. Held, V. Eyert, D. Vollhardt, and V. I. Anisimov, *Phys. Rev. B* **70**, 205116 (2004).
- [11] G. Panaccione, M. Altarelli, A. Fondacaro, A. Georges, S. Huotari, P. Lacovig, A. Lichtenstein, P. Metcalf, G. Monaco, F. Offi, L. Paolasini, A. Poteryaev, O. Tjernberg, and M. Sacchi, *Phys. Rev. Lett.* **97**, 116401 (2006).
- [12] A. I. Poteryaev, J. M. Tomczak, S. Biermann, A. Georges, A. I. Lichtenstein, A. N. Rubtsov, T. Saha-Dasgupta, and O. K. Andersen, *Phys. Rev. B* **76**, 085127 (2007).
- [13] L. Baldassarre, A. Perucchi, D. Nicoletti, A. Toschi, G. Sangiovanni, K. Held, M. Capone, M. Ortolani, L. Malavasi, M. Marsi, P. Metcalf, P. Postorino, and S. Lupi, *Phys. Rev. B* **77**, 113107 (2008); J. M. Tomczak and S. Biermann, *J. Phys. Condens. Matter* **21**, 064209 (2009); F. Rodolakis, J.-P. Rueff, M. Sikora, I. Alliot, J.-P. Itié, F. Baudelet, S. Ravy, P. Wzietek, P. Hansmann, A. Toschi, M. W. Haverkort, G. Sangiovanni, K. Held, P. Metcalf, and M. Marsi, *Phys. Rev. B* **84**, 245113 (2011).
- [14] S.-K. Mo, J. D. Denlinger, H.-D. Kim, J.-H. Park, J. W. Allen, A. Sekiyama, A. Yamasaki, K. Kadono, S. Suga, Y. Saitoh, T. Muro, P. Metcalf, G. Keller, K. Held, V. Eyert, V. I. Anisimov, and

- D. Vollhardt, *Phys. Rev. Lett.* **90**, 186403 (2003); S.-K. Mo, H.-D. Kim, J. D. Denlinger, J. W. Allen, J.-H. Park, A. Sekiyama, A. Yamasaki, S. Suga, Y. Saitoh, T. Muro, and P. Metcalf, *Phys. Rev. B* **74**, 165101 (2006).
- [15] S. Lupi, L. Baldassarre, B. Mansart, A. Perucchi, A. Barinov *et al.*, *Nat. Commun.* **1**, 105 (2010).
- [16] I. Leonov, N. Binggeli, Dm. Korotin, V. I. Anisimov, N. Stojić, and D. Vollhardt, *Phys. Rev. Lett.* **101**, 096405 (2008); I. Leonov, Dm. Korotin, N. Binggeli, V. I. Anisimov, and D. Vollhardt, *Phys. Rev. B* **81**, 075109 (2010).
- [17] S. Baroni, S. de Gironcoli, A. Dal Corso, and P. Giannozzi, *Rev. Mod. Phys.* **73**, 515 (2001); P. Giannozzi, S. Baroni, N. Bonini, M. Calandra, R. Car *et al.*, *J. Phys. Condens. Matter* **21**, 395502 (2009).
- [18] V. I. Anisimov, D. E. Kondakov, A. V. Kozhevnikov, I. A. Nekrasov, Z. V. Pchelkina, J. W. Allen, S.-K. Mo, H.-D. Kim, P. Metcalf, S. Suga, A. Sekiyama, G. Keller, I. Leonov, X. Ren, and D. Vollhardt, *Phys. Rev. B* **71**, 125119 (2005); G. Trimarchi, I. Leonov, N. Binggeli, Dm. Korotin, and V. I. Anisimov, *J. Phys. Condens. Matter* **20**, 135227 (2008); Dm. Korotin, A. V. Kozhevnikov, S. L. Skornyakov, I. Leonov, N. Binggeli, V. I. Anisimov, and G. Trimarchi, *Eur. Phys. J. B* **65**, 91 (2008).
- [19] P. Werner, A. Comanac, L. de'Medici, M. Troyer, and A. J. Millis, *Phys. Rev. Lett.* **97**, 076405 (2006); E. Gull, A. J. Millis, A. I. Lichtenstein, A. N. Rubtsov, M. Troyer, and P. Werner, *Rev. Mod. Phys.* **83**, 349 (2011).
- [20] We here employ the density-density approximation of the local Coulomb interaction between the $V t_{2g}$ electrons.
- [21] A. Jayaraman, D. B. McWhan, J. P. Remeika, and P. D. Dernier, *Phys. Rev. B* **2**, 3751 (1970); P. Limelette, A. Georges, D. Jerome, P. Wzietek, P. Metcalf, and J. M. Honig, *Science* **302**, 89 (2003).
- [22] H. Fujiwara, A. Sekiyama, S.-K. Mo, J. W. Allen, J. Yamaguchi, G. Funabashi, S. Imada, P. Metcalf, A. Higashiya, M. Yabashi, K. Tamasaku, T. Ishikawa, and S. Suga, *Phys. Rev. B* **84**, 075117 (2011).
- [23] W. F. Brinkman and T. M. Rice, *Phys. Rev. B* **2**, 4302 (1970).
- [24] For a review, see, e.g., L. V. Pourovskii, B. Amadon, S. Biermann, and A. Georges, *Phys. Rev. B* **76**, 235101 (2007); K. Haule, *ibid.* **75**, 155113 (2007); B. Amadon, F. Lechermann, A. Georges, F. Jollet, T. O. Wehling, and A. I. Lichtenstein, *ibid.* **77**, 205112 (2008); M. Aichhorn, L. Pourovskii, V. Vildosola, M. Ferrero, O. Parcollet, T. Miyake, A. Georges, and S. Biermann, *ibid.* **80**, 085101 (2009); H. Park, A. J. Millis, and C. A. Marianetti, *ibid.* **90**, 235103 (2014).
- [25] G. Kotliar, S. Murthy, and M. J. Rozenberg, *Phys. Rev. Lett.* **89**, 046401 (2002); S. R. Hassan, A. Georges, and H. R. Krishnamurthy, *ibid.* **94**, 036402 (2005).
- [26] J.-H. Park, L. H. Tjeng, A. Tanaka, J. W. Allen, C. T. Chen, P. Metcalf, J. M. Honig, F. M. F. de Groot, and G. A. Sawatzky, *Phys. Rev. B* **61**, 11506 (2000).
- [27] P. Pfalzer, G. Obermeier, M. Klemm, S. Horn, and M. L. denBoer, *Phys. Rev. B* **73**, 144106 (2006); S. Populoh, P. Wzietek, R. Gohier, and P. Metcalf, *ibid.* **84**, 075158 (2011); J. Köndel, P. Pontiller, C. Müller, G. Obermeier, Z. Liu, A. A. Nateprov, A. Hörner, A. Wixforth, S. Horn, and R. Tidecks, *Appl. Phys. Lett.* **102**, 101904 (2013).
- [28] D. B. McWhan, J. P. Remeika, T. M. Rice, W. F. Brinkman, J. P. Maita, and A. Menth, *Phys. Rev. Lett.* **27**, 941 (1971); S. A. Carter, T. F. Rosenbaum, P. Metcalf, J. M. Honig, and J. Spalek, *Phys. Rev. B* **48**, 16841 (1993).